

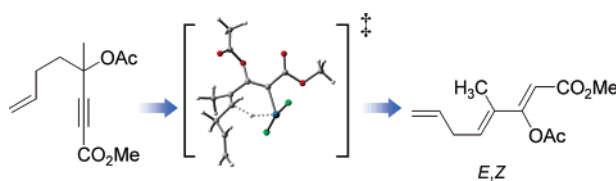
## DFT-Based Mechanism for the Unexpected Formation of Dienes in the PtCl<sub>2</sub> Isomerization of Propargylic Acetates: Examples of Inhibition of the Rautenstrauch Process

Elena Soriano\*<sup>†</sup> and José Marco-Contelles<sup>‡</sup>

Laboratorio de Resonancia Magnética, Instituto de Investigaciones Biomédicas (CSIC), C/Arturo Duperier 4, 28029 Madrid, Spain, and Laboratorio de Radicales Libres, IQOG (CSIC), C/Juan de la Cierva 3, 28006 Madrid, Spain

esoriano@iib.uam.es

Received November 7, 2006



The reactivity of the Pt(II)-mediated processes of unsaturated compounds strongly depends on the substrate structure, and the catalytic activation process may follow different reaction paths, such as skeletal rearrangements, cyclizations, and isomerizations. Herein, we analyze and report the striking effect of an ester group as an alkyne substituent on the reactivity of propargylic enynes, which has been shown to inhibit the expected Rautenstrauch process. The computed results agree with experimental evidence and provide a comprehensible rationalization.

### Introduction

The use of late transition metal complexes as soft Lewis acids and catalysts in organic synthesis has greatly increased in the past few years.<sup>1</sup> This methodology allows rearrangements of unsaturated structures providing efficient access to complex frameworks. Complexation of alkynes to soft noble metal complexes such as PtCl<sub>2</sub>, Au(I)-salts, or AuCl<sub>3</sub> triggers nucleophilic attack by alkenes, arenes, ethers, or carbonyl groups that allows the transformation of polyunsaturated precursors into important synthetic building blocks.<sup>2–6</sup> Thus, platinum chloride has been recognized to induce highly selective skeletal rearrangements and cycloisomerizations and, hence, has become

a widely used catalyst.<sup>7</sup> These Pt(II)-catalyzed processes are inherently atom economical, result in a significant increase in structural complexity, and are operationally simple and safe. In this context, the readily available propargylic esters<sup>8</sup> have been shown to afford inspiring cyclic skeletons for the synthesis of natural products through the Rautenstrauch rearrangement.<sup>5,9–13</sup>

(4) (a) Trost, B. M.; Krische, M. J. *Synlett* **1998**, 1–16. (b) Trost, B. M.; Krische, M. J. *J. Am. Chem. Soc.* **1999**, *121*, 6131–6141. (c) Takayama, Y.; Okamoto, S.; Sato, F. *J. Am. Chem. Soc.* **1999**, *121*, 3559–3560. (d) Trost, B. M.; Toste, F. D. *J. Am. Chem. Soc.* **2000**, *122*, 714–715. (e) Trost, B. M.; Pedregal, C. *J. Am. Chem. Soc.* **1992**, *114*, 7292–7294. (f) Lei, A.; Waldkirch, J. P.; He, M.; Zhang, X. *Angew. Chem., Int. Ed.* **2002**, *41*, 4526–4529.

(5) (a) Mainetti, E.; Mouries, V.; Fensterbank, L.; Malacria, M.; Marco-Contelles, J. *Angew. Chem., Int. Ed.* **2002**, *41*, 2132–2135. (b) Anjum, S.; Marco-Contelles, J. *Tetrahedron* **2005**, *61*, 4793–4803.

(6) Some Pt- and Au-catalyzed transformations in protic media reported in the literature are likely to be a Brønsted acid-catalyzed process. Recent papers supporting the notion that many M-X-catalyzed reactions are actually catalyzed by H-X that is produced from the metal halide and adventitious water: (a) Rosenfeld, D. C.; Shekhar, S.; Takemiya, A.; Utsunomiya, M.; Hartwig, J. F. *Org. Lett.* **2006**, *8*, 4179–4182. (b) Li, Z.; Zhang, J.; Brouwer, C.; Yang, C-G.; Reich, N. W.; He, C. *Org. Lett.* **2006**, *8*, 4175–4178. (c) Rhee, J. U.; Krische, M. J. *Org. Lett.* **2005**, *7*, 2493–2495. We thank one referee for calling our attention to this interesting proposal.

(7) Pioneering studies: (a) Chatani, N.; Furukawa, N.; Sakurai, H.; Murai, S. *Organometallics* **1996**, *15*, 901–903. (b) Blum, J.; Beer-Kraft, H.; Badrieh, H. *J. Org. Chem.* **1995**, *60*, 5567–5569.

(8) Tsuji, J.; Mandai, T. *Angew. Chem., Int. Ed.* **1995**, *34*, 2589–2612.

\* Corresponding author. Tel.: 34 00 913987320.

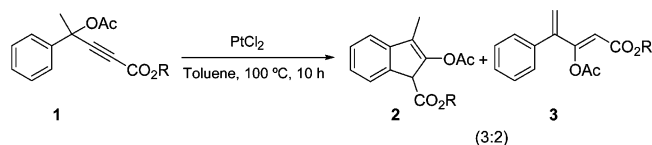
<sup>†</sup> Instituto de Investigaciones Biomédicas.

<sup>‡</sup> Laboratorio de Radicales Libres.

(1) For recent reviews, see: (a) Lloyd-Jones, G. C. *Org. Biomol. Chem.* **2003**, *1*, 215–236. (b) Méndez, M.; Mamane, V.; Fürstner, A. *Chemtracts* **2003**, *16*, 397–425. (c) Aubert, C.; Buisine, O.; Malacria, M. *Chem. Rev.* **2002**, *102*, 813–834.

(2) (a) Bruneau, C. *Angew. Chem., Int. Ed.* **2005**, *44*, 2328–2334. (b) Fürstner, A.; Szillat, H.; Stelzer, F. *J. Am. Chem. Soc.* **2000**, *122*, 6785–6786. (c) Méndez, M.; Muñoz, M. P.; Nevado, C.; Cárdenas, D. J.; Echavarren, A. M. *J. Am. Chem. Soc.* **2001**, *123*, 10511–10520.

(3) (a) Diver, S. T.; Giessent, A. *J. Chem. Rev.* **2004**, *104*, 1317–1382. (b) Mori, M. In *Topics in Organometallic Chemistry*; Fürstner, A., Ed.; Springer-Verlag: Berlin, 1998; Vol. 1, pp 133–154. (c) Fürstner, A. *Angew. Chem., Int. Ed.* **2000**, *39*, 3012–3043. (d) Poulsen, C. S.; Madsen, R. *Synthesis* **2003**, 1–18.

**SCHEME 1. Pentannulation Reaction on Aryl Propargylic Acetates**


Recently, Sarpong and co-workers<sup>14</sup> reported Pt-catalyzed pentannulations of aryl propargylic esters for the synthesis of indenenes (Scheme 1),<sup>15</sup> a methodology previously applied to related 1,6- and 1,5-enynes for the synthesis of bicyclic [n.1.0] derivatives (Rautenstrauch cyclopropanation),<sup>5,10–12</sup> and where the electron-rich phenyl ring replaces the alkene moiety. Besides the expected intramolecular hydroarylation product **2** (Rautenstrauch pentannulation product), a diene **3** was also obtained in a significant yield (2/3 = 60:40).

To account for the pentannulation, Sarpong and co-workers proposed a mechanism, shown in Scheme 2, involving an initial 5-*exo*-dig cyclization of the ester carbonyl oxygen onto the activated alkyne, followed by C–O bond cleavage and an irreversible formal C–H insertion.<sup>14</sup> This mechanistic scheme is closely related to those initially proposed by Marco-Contelles and Malacria<sup>5a</sup> and Uemura et al.<sup>15a</sup> Toste et al. also suggested initial migration of the ester group for the Au(I)-mediated cycloisomerization of acyclic 1,4-enynes, although they put forward a concerted ester shift/cyclization, with no formation of metal carbenes,<sup>13</sup> to justify the stereochemical course of the rearrangement.<sup>16</sup>

In their report on aryl propargyl esters, Sarpong et al. alluded to a mechanism presented earlier by Malacria<sup>17</sup> (Scheme 3) for the unexpected formation of the diene **3**. This type of byproduct has also been isolated in the Pt-mediated isomerization of 1,6-enynes, as described by Malacria et al.<sup>17</sup> and Marco-Contelles et al. (Scheme 4).<sup>18</sup> To the best of our knowledge, this process has been reported only for propargylic acetates bearing an ester group at the alkyne site and promoted by PtCl<sub>2</sub>.<sup>15</sup>

(9) For pioneering works, see: (a) Rautenstrauch, V. *J. Org. Chem.* **1984**, *49*, 950–952. The same cyclization, but catalyzed by ZnCl<sub>2</sub>, was described some years before. (b) Strickler, H.; Davis, J. B.; Ohloff, G. *Helv. Chim. Acta.* **1976**, *59*, 1328–1332.

(10) (a) Blaszykowski, C.; Harrak, Y.; Gonçalves, M. H.; Cloarec, J. M.; Dhimane, A. L.; Fensterbank, L.; Malacria, M. *Org. Lett.* **2004**, *6*, 3771–3774. (b) Harrak, Y.; Blaszykowski, C.; Bernard, M.; Cariou, K.; Mainetti, E.; Mouriès, V.; Dhimane, A. L.; Fensterbank, L.; Malacria, M. *J. Am. Chem. Soc.* **2004**, *126*, 8656–8657. (c) For Au(I)-induced cycloisomerization of propargyl acetates, see: Marion, N.; de Frémont, P.; Lemièrre, G.; Stevens, E. D.; Fensterbank, L.; Malacria, M.; Nolan, S. P. *Chem. Commun.* **2006**, 2048–2050.

(11) (a) Fürstner, F.; Hannen, P. *Chem. Commun.* **2004**, 2546–2547. (b) Mamane, V.; Gress, T.; Krause, H.; Fürstner, A. *J. Am. Chem. Soc.* **2004**, *126*, 8654–8655. (c) Fürstner, A.; Hannen, P. *Chem.–Eur. J.* **2006**, *12*, 3006–3019.

(12) Fehr, C.; Galindo, J. *Angew. Chem., Int. Ed.* **2006**, *45*, 2901–2904.

(13) Shi, X.; Gorin, D. J.; Toste, F. D. *J. Am. Chem. Soc.* **2005**, *127*, 5802–5803.

(14) Prasad, B. A. B.; Yoshimoto, F. K.; Sarpong, R. *J. Am. Chem. Soc.* **2005**, *127*, 12468–12469. The authors observed that PtCl<sub>2</sub>(PPh<sub>3</sub>)<sub>2</sub> as a precatalyst gave better selectivity for the hydroarylation product than PtCl<sub>2</sub>.

(15) For the ruthenium-catalyzed formation of indenenes from aryl propargyl acetates, see: (a) Miki, K.; Ohe, K.; Uemura, S. *J. Org. Chem.* **2003**, *68*, 8505–8513. For Au-catalyzed formation of indenenes from aryl propargyl acetates, see: (b) Marion, N.; Díez-González, S.; de Frémont, P.; Noble, A. R.; Nolan, S. P. *Angew. Chem., Int. Ed.* **2006**, *45*, 3647–3650.

(16) Nieto-Faza, O.; Silva-López, C.; Álvarez, R.; de Lera, A. R. *J. Am. Chem. Soc.* **2006**, *128*, 2434–2437.

(17) Cariou, K.; Mainetti, E.; Fensterbank, L.; Malacria, M. *Tetrahedron* **2004**, *60*, 9745–9755.

For the equivalent reaction product **7** formed by exposure of the 1,6-enyne **6** to Pt(II), Malacria et al. have suggested the mechanism proceeds via nucleophilic attack of the ester at the alkyne followed by a concerted Pt-assisted H abstraction/C–O bond cleavage (Scheme 3). In their paper, details on the precise stereochemistry of **7** were not supplied.<sup>17</sup> For the enyne precursor **8**, which is closely related to **6**, the *E* configuration at the C<sub>4</sub>=C<sub>5</sub> bond in the product **9** has been unequivocally assigned by NMR experiments, implying a diastereoselective H-elimination process (Scheme 4).<sup>18</sup>

The main questions arising from these results refer to the role played by the electron-withdrawing group at the terminus of the alkyne on the inhibition of the expected Rautenstrauch cycloisomerization and also on the competing and remarkably diastereoselective isomerization. The purpose of this work is to address these points by means of DFT calculations in the hopes of assisting in the design of more efficient synthetic protocols.

**Results and Discussion**

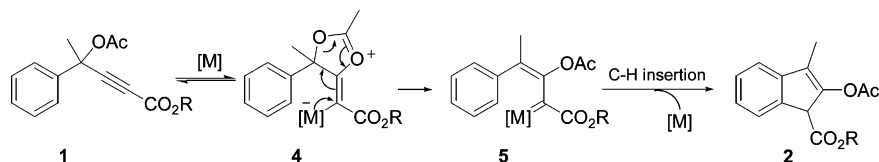
The mechanism proposed by Sarpong for the Pt-catalyzed pentannulation of **1** initially involves the potentially reversible 5-*exo*-dig cyclization of the propargylic ester oxygen onto the activated  $\eta^2$ -complexed alkyne to form **4** (Scheme 2). The metal may adopt two orientations relative to the migrating ester, *Z* and *E*. According to our calculations for **1** (and backed up by calculations on simple 1,4-enynes, see Supporting Information for details), the reactant complex evolves into the *E*-alkene through the transition structure **TS1** by anti-nucleophilic attack of the oxygen lone pair onto the complexed alkyne, which initiates the formation of a  $\sigma$ -metal–carbon bond (1.981 Å, see Figure 1).<sup>19</sup>

The formation of the planar oxacycle **4** from the reactant complex **1**–PtCl<sub>2</sub> takes places with a very low-energy barrier (3.86 kcal mol<sup>–1</sup> in toluene and 4.82 kcal mol<sup>–1</sup> in the gas phase) and is moderately exothermic (–16.32 kcal mol<sup>–1</sup> in toluene). This activation energy is considerably lower than that computed for a simple 1,4-enyne lacking substituents on the alkyne group (7.60 kcal mol<sup>–1</sup> for the *E* isomer in the gas phase, see Supporting Information). The terminal ester moiety induces electronic factors that could enhance the electrophilic character at the internal carbon position, as revealed by Natural Population Analysis (NPA) charges. In a comparison with the unsubstituted simple 1,4-enyne (see Supporting Information), the alkyne ester increases the positive charge at the internal alkyne carbon (+0.004 for a trans complexed unsubstituted alkyne vs +0.074 for **1**–PtCl<sub>2</sub>; for the metal-free unsubstituted acetylene –0.059 vs +0.045 bearing a CO<sub>2</sub>Me attached), which makes the 5-*exo*-dig cyclization of the ester oxygen more favorable from a kinetic point of view.

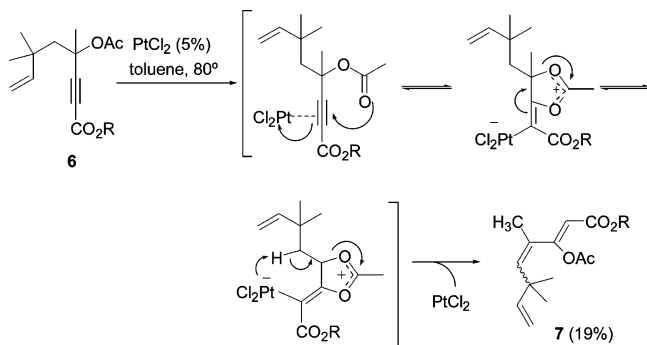
Intermediate **4** evolves by C–O bond cleavage to the Pt–carbenoid **5** through the transition structure **TS2**. Then, the metallo–carbenoid **5** cyclizes through **TS3** (activation barrier of 15.61 kcal mol<sup>–1</sup>), leading to **10**. This intermediate shows a

(18) Marco-Contelles, J.; Arroyo, N.; Anjum, S.; Mainetti, E.; Marion, N.; Cariou, K.; Lemièrre, G.; Mouriès, V.; Fensterbank, L.; Malacria, M. *Eur. J. Org. Chem.* **2006**, 4618–4633. The process furnished a complex mixture (polymerization and other unknown byproducts, TLC analysis) from which the product **9** could be characterized and isolated in only 11% yield.

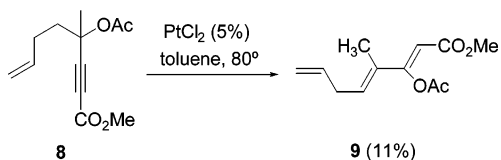
(19) This effect differs from that observed for longer enynes (1,5- and 1,6-enynes) since the *Z* isomer appears to be favored mainly due to the more favorable final cyclopropanation. See ref 23.

SCHEME 2. Proposed Mechanism for the Formation of Compound 2<sup>a</sup><sup>a</sup> Ref 14.

## SCHEME 3



## SCHEME 4



structure resembling the Wheland intermediate, where the *ipso*-carbon atom exhibits an evident sp<sup>3</sup> hybridization, providing evidence for the full  $\sigma$  character of this species,<sup>20</sup> and the Pt–C bond is longer than for the previous carbene intermediate (2.042 Å for **10** vs 1.875 Å for **5**). This mechanistic scheme is comparable to that proposed by Lera et al. for the Au(I)-induced cycloisomerization of nonaromatic precursors.<sup>16</sup> After a thorough search, we could not locate a transition state connecting **4** and the cyclized adduct **10**. Thus, it does not appear that the cyclization is concerted, as was postulated to occur in related systems.<sup>13</sup> Figure 1 depicts the free energy profile computed in solution (toluene) for the transformation of **1** into **10**.

The formation of the diene **3** (Scheme 1) from **1** also implies a [1,2]-acyl migration, which should take place via an *E* intermediate **11** since the anti-disposition of the two forming  $\sigma$  bonds warrants the *Z* configuration of the diester-substituted double bond in **3**. Hence, the formation of the open-chain diene **3** as well as the cyclized product **2** suggests a bifurcation of the synthetic pathway. A conformer with the proper arrangement between the catalyst and the methyl group, **5'** (Scheme 5), was found. This alternative intermediate may undergo a  $\delta$ -H elimination leading to **11**. This step is kinetically (by 0.8 kcal mol<sup>-1</sup>) and thermodynamically (by 10.5 kcal mol<sup>-1</sup>) less favored than the expected Rautenstrauch process, as can be seen in Figure 1, which could account for the observed product ratio. We can then ascribe the fact that this isomerization reaction takes place mediated by PtCl<sub>2</sub>, but not by Au(I), which normally promotes similar transformations,<sup>11b,12,21</sup> to gold's low tendency for hydride elimination.<sup>22</sup>

The sequence of events detailed previously, where **1** is transformed into **10**, differs from that proposed by us for the formation of cyclopropyl derivatives from 1,5- and 1,6-enynes

(Rautenstrauch cyclopropanation), where the C–C bond forming event precedes the migration of the propargylic ester.<sup>23</sup> Therefore, we suspect that the tether length connecting the reactive alkene and alkyne units might guide the reaction pathway to be followed. In accord with the suggested mechanism for the Rautenstrauch cyclopropanation, precursor **8** (Scheme 4) should evolve through 6-*endo*-dig cyclopropanation and stepwise[1,2]-acyl migration events to yield the expected bicyclo[4.1.0]hept-4-enol ester (Scheme 6). Many recent reports have established the versatility and success of the transformation of 1,6-enynes into the bicyclo[4.1.0]hept-4-ene framework, which is efficiently mediated by Pt(II) and also by Au(I) and Au(III).<sup>5,10–12</sup> The fact that an ester group at the acetylenic position inhibits the expected Rautenstrauch cyclopropanation (Scheme 6) demands further analysis. Computational investigation of the cyclopropanation step reveals an energy barrier for the formation of the cyclopropyl intermediate **12** of 10.78 kcal mol<sup>-1</sup> in the gas phase (10.41 kcal mol<sup>-1</sup> in toluene), which is 2.07 kcal mol<sup>-1</sup> higher than that computed for an unsubstituted 1,6-enyne.<sup>23</sup> The acetylenic substitution gives rise to a slight displacement of the catalyst to relieve steric hindrance, inducing a less efficient alkyne activation in the reactant complex **8**–PtCl<sub>2</sub>. This effect is enhanced by substitution at the propargylic position. In support of this, anomalous results have also been reported for other enyne precursors with methyl or phenyl substituents when a quaternary propargylic center was present.<sup>11c</sup> The alkyne group is more symmetrically coordinated to the metal center in the  $\eta^2$ -reactant complex **8**–PtCl<sub>2</sub> as compared with unsubstituted precursors, allowing a slightly shorter Pt–C<sub>2</sub> interaction (2.12 Å vs 2.18 Å for unsubstituted 1,6-enyne<sup>23a</sup>). As a consequence, the catalyst enhances the polarization on the bonded alkyne, where the internal carbon becomes more electrophilic than for the unsubstituted alkyne (NPA charges +0.093 and +0.035,<sup>23a</sup> respectively). Under these circumstances, a [1,2]-acyl shift emerges as a competitive path.

Following the reaction mechanism described for the transformation of **1** into **3** (Scheme 5), the stepwise acyl migration takes place through two transition structures involving activation barriers of 4.01 and 8.33 kcal mol<sup>-1</sup>, respectively (Figure 2), yielding the intermediate structure **14** (Scheme 6). At this point,

(20) Hubig, S. M.; Kochi, J. K. *J. Org. Chem.* **2000**, *65*, 6807–6818.(21) (a) Staben, S. T.; Kennedy-Smith, J. J.; Huang, D.; Corkey, B. K.; Lalonde, R. L.; Toste, F. D. *Angew. Chem., Int. Ed.* **2006**, *45*, 5991–5994. (b) Nieto-Oberhuber, C.; López, S.; Muñoz, M. P.; Jiménez-Núñez, E.; Buñuel, E.; Cárdenas, D. J.; Echavarren, A. M. *Chem.–Eur. J.* **2006**, *12*, 1694–1702. (c) Johansson, M. J.; Gorin, D. J.; Staben, S. T.; Toste, F. D. *J. Am. Chem. Soc.* **2005**, *127*, 18002–18003. (d) Hashmi, A. S. K.; Weyrauch, J. P.; Frey, W.; Bats, J. W. *Org. Lett.* **2004**, *6*, 4391–4394. (e) Nieto-Oberhuber, C.; Muñoz, M. P.; Buñuel, E.; Nevado, C.; Cárdenas, D. J.; Echavarren, A. M. *Angew. Chem., Int. Ed.* **2004**, *116*, 2402–2406. (f) Luzung, M. R.; Markham, J. P.; Toste, F. D. *J. Am. Chem. Soc.* **2004**, *126*, 10858–10859.(22) Ma, S.; Yu, S.; Gu, Z. *Angew. Chem., Int. Ed.* **2006**, *45*, 200–203.(23) (a) Soriano, E.; Ballesteros, P.; Marco-Contelles, J. *Organometallics* **2005**, *24*, 3182–3191. (b) Soriano, E.; Marco-Contelles, J. *J. Org. Chem.* **2005**, *70*, 9345–9353.

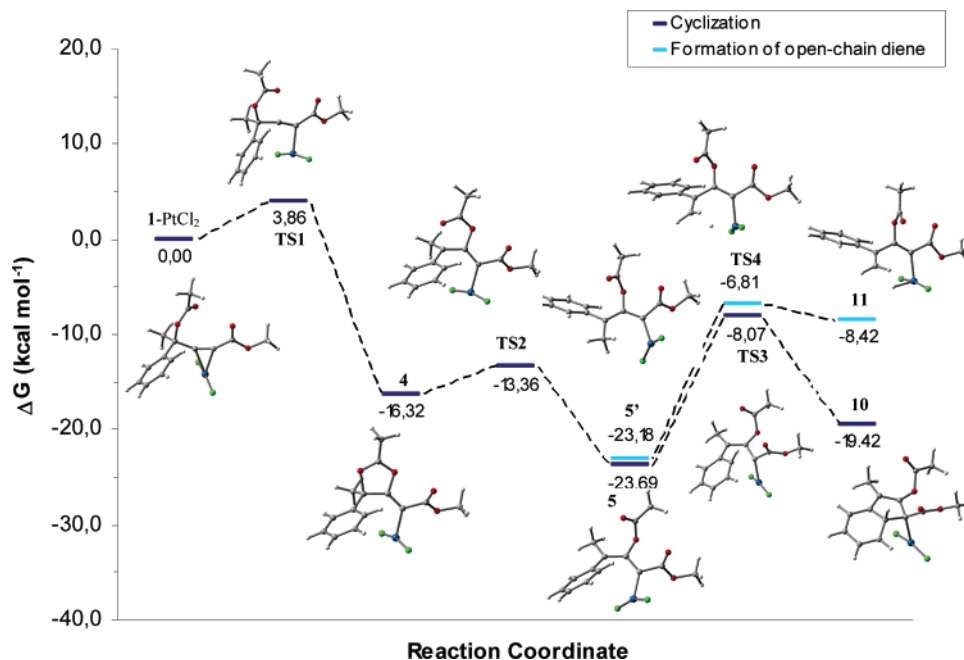
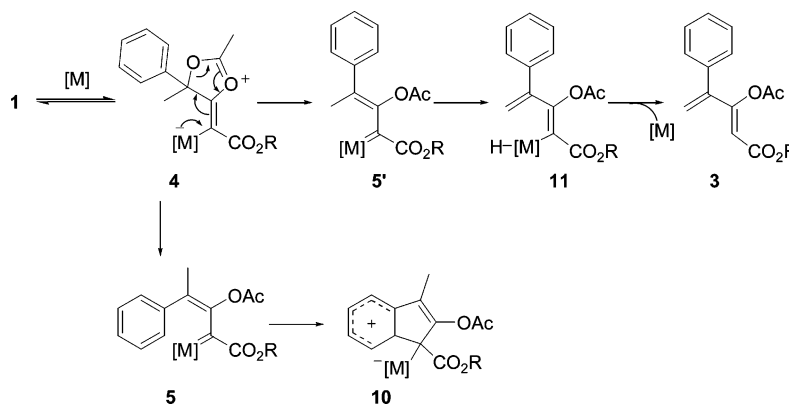
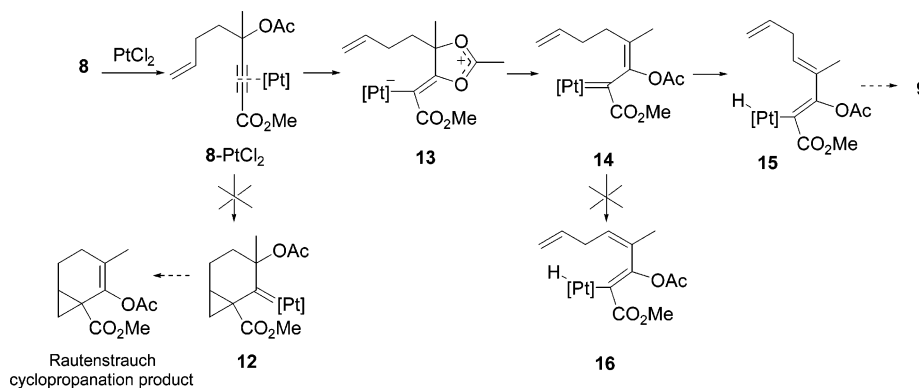


FIGURE 1. Computed free-energy profile in solution (toluene) for the  $\text{PtCl}_2$ -catalyzed transformation of alkyne **1** into **10** and **11**.

#### SCHEME 5



#### SCHEME 6



a diastereoselective Pt-assisted hydrogen abstraction to form a dienylplatinum hydride **15** that undergoes reductive elimination would lead to the observed triene **9** (Scheme 6). The isomeric dienylplatinum hydride **16**, which would yield the *E* ( $\text{C}_4=\text{C}_5$ ) isomer of compound **9**, was not detected experimentally.<sup>18</sup> A closer inspection of the metallo-carbenoid **14** may provide insights into this selectivity.

Steric crowding in the T-shaped Pt complex **14** induces slight steric interactions between the alkyl chain and the catalyst, which results in a conformational preference of  $0.56 \text{ kcal mol}^{-1}$  for **14** relative to **14'** (the conformer that gives rise to the alternative H abstraction). However, this energy difference is too low to explain the stereoselective Pt-assisted H abstraction, and other factors must come into play. The transition structure involved



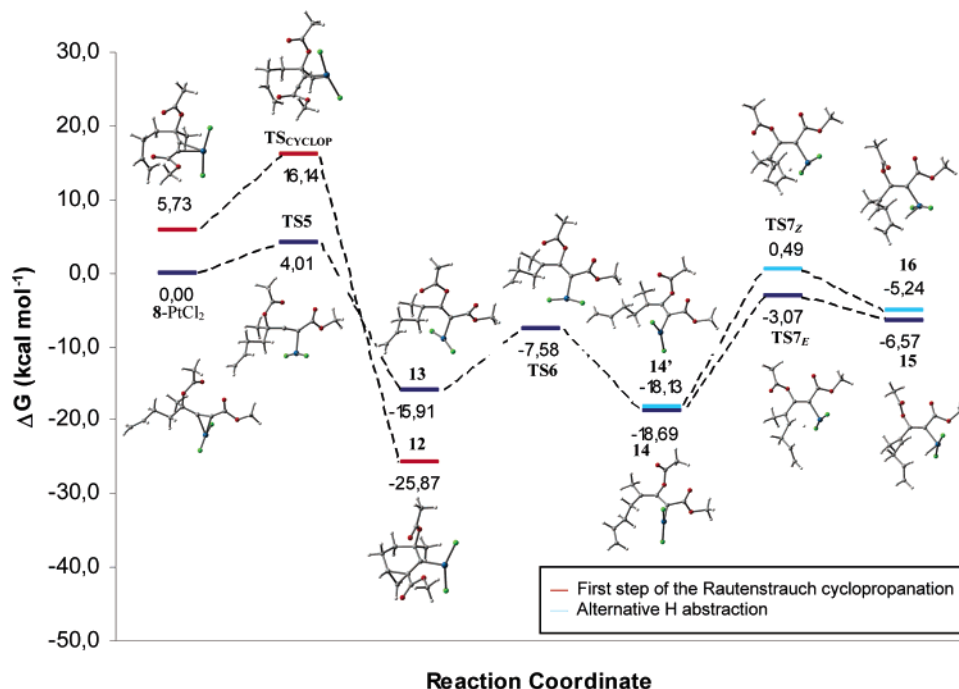


**FIGURE 2.** Computed free-energy profile in solution (toluene) for the PtCl<sub>2</sub>-catalyzed transformation of enyne **8** following different paths. Relative free-energy values are given in kcal mol<sup>-1</sup>.

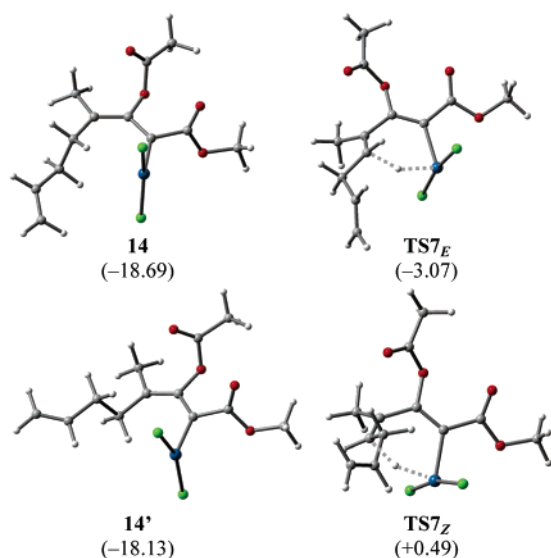


**FIGURE 3.** Optimized intermediates and transition structures in the Pt-mediated abstraction step. Free energy differences relative to reactant complex **8**-PtCl<sub>2</sub> are given in kcal mol<sup>-1</sup>.

in the formation of the trans adduct (**TS7<sub>E</sub>**) to form the dienylplatinum hydride **15** (Figure 3) is stabilized by 3.56 kcal mol<sup>-1</sup> over that (**TS7<sub>Z</sub>**) affording the cis adduct **16**. According to NBO second-order perturbation theory analysis, the lack of steric interactions in **TS7<sub>E</sub>** allows an effective interaction between the  $\pi$  bonding C<sup>a</sup>-C<sup>b</sup> and  $\pi$  antibonding C<sup>c</sup>-C<sup>d</sup> orbitals and between the  $\pi$  bonding C<sup>c</sup>-C<sup>d</sup> and the  $\pi$  antibonding C<sup>a</sup>-C<sup>b</sup>, involving delocalization energies ( $E_2$ ) of 7.23 and 9.36 kcal mol<sup>-1</sup>, respectively (Figure 4). Conversely, in **TS7<sub>Z</sub>**, the steric crowding at the transition metal center gives rise to a slight opening of the C<sup>a</sup>-C<sup>b</sup>-C<sup>c</sup>-C<sup>d</sup> dihedral angle, which induces less effective orbital interactions (4.66 and 8.20 kcal mol<sup>-1</sup>). These

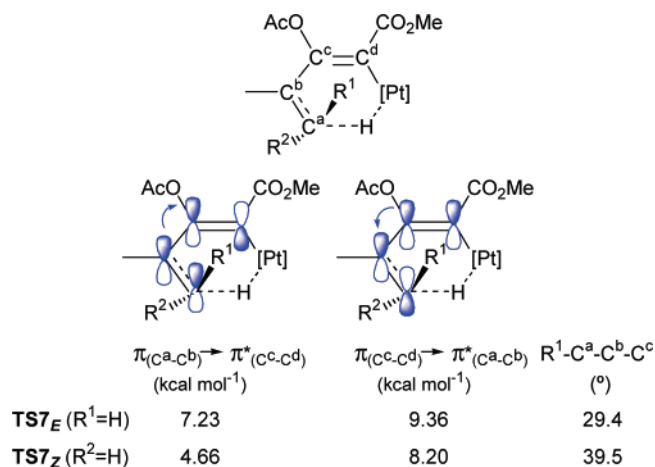


**FIGURE 4.** Significant donor-acceptor (bonding-antibonding) interactions in the NBO basis for the possible transition structures **TS3<sub>E</sub>** and **TS3<sub>Z</sub>** involved in the Pt-assisted H-abstraction step. The corresponding second-order perturbation energies are given in kcal mol<sup>-1</sup>.

effects would result in a lower energy barrier for the formation of the trans adduct and explain the selectivity found in the experimental isomerization of enyne **8** to triene **9** (Scheme 4).<sup>18</sup>

## Conclusion

We have studied the role of an acetylenic ester in the course of the Pt(II)-mediated cycloisomerization of propargylic acetates. This electron-withdrawing substituent at the terminus of the alkyne induces steric and, more importantly, electronic effects that inhibit the expected Rautenstrauch process and forces the process to follow an alternative path involving catalyst-mediated hydride abstraction. The mechanisms of the usual and competing paths have been analyzed in detail, and the computed results

agree with the available experimental results. We have accounted for the diastereoselectivity found in the Pt-assisted hydride abstraction by means of NBO analysis, concluding that steric interactions in the transition structure gives rise to different hyperconjugation interaction energies that, in turn, determine the magnitude of the energy barrier for the rate-limiting H-abstraction step.

### Computational Methods

Calculations have been carried out using the Gaussian03 program.<sup>24</sup> All the structures have been optimized at the DFT level by means of the B3LYP functional.<sup>25</sup> The 6-31G(d) basis set has been applied for all atoms except Pt, which has been described by the LANL2DZ basis set,<sup>26</sup> where the innermost electrons are replaced by a relativistic ECP and the valence electrons are

explicitly treated by a double- $\zeta$  basis set. The optimized geometries were characterized by harmonic analysis, and the nature of the stationary points was determined according to the number of negative eigenvalues of the Hessian matrix. The intrinsic reaction coordinate (IRC) pathways<sup>27a</sup> from the transition structures have been followed using a second-order integration method,<sup>27b</sup> to verify the connections of the first-order saddle points with the correct local minima. Zero-point vibration energy (ZPVE) and thermal corrections (at 298 K, 1 atm) to the energy have been estimated based on the frequency calculations.

The solvation energies were calculated on the gas-phase optimized structures with the Polarizable Continuum Model, PCM,<sup>28</sup> as implemented in Gaussian03, and using the UAKS radii.<sup>29</sup> A relative permittivity of 2.379 was assumed to simulate toluene as the solvent that was used experimentally.

Natural bond orbital (NBO) analyses<sup>30</sup> have been performed by the module NBO v.3.1 implemented in Gaussian03 to evaluate the NPA charges and hyperconjugation effects.

**Acknowledgment.** We thank the referees for their useful comments and suggestions.

**Supporting Information Available:** Complete ref 24, additional results for the mechanism of the Rautenstrauch pentannulation for 1,4-enynes, and atomic coordinates for the computed structures. This material is available free of charge via the Internet at <http://pubs.acs.org>.

JO0622983

(24) Frisch, M. J. et al. *Gaussian 03*, revision B.03; Gaussian, Inc.: Pittsburgh PA, 2003. See Supporting Information.

(25) (a) Lee, C.; Yang, W.; Parr, R. *Phys. Rev. B* **1988**, *37*, 785–789.

(b) Becke, A. *J. Chem. Phys.* **1993**, *98*, 5648–5652.

(26) Hay, P. J.; Wadt, W. R. *J. Chem. Phys.* **1985**, *82*, 270–283.

(27) (a) Fukui, K. *Acc. Chem. Res.* **1981**, *14*, 363–368. (b) González, C.; Schlegel, H. B. *J. Phys. Chem.* **1990**, *94*, 5523–5527.

(28) (a) Tomasi, J.; Persico, M. *Chem. Rev.* **1994**, *94*, 2027–2094. (b) Cossi, M.; Scalmani, G.; Rega, N.; Barone, V. *J. Chem. Phys.* **2002**, *117*, 43–54.

(29) Barone, V.; Cossi, M. *J. Phys. Chem. A* **1998**, *102*, 1995–2001.

(30) (a) Reed, A. E.; Weinhold, F. *J. Chem. Phys.* **1983**, *78*, 4066–4073. (b) Reed, A. E.; Curtiss, L. A.; Weinhold, F. *Chem. Rev.* **1988**, *88*, 899–926.